

Inductive Effects in Neutral Pentacoordinated Silicon Compounds Containing a Si ← N Dative Bond. A Theoretical Study

Josep M. Anglada,^{*,†} Carles Bo,[‡] Josep M. Bofill,^{*,§} Ramon Crehuet,[†] and Josep M. Poblet^{*,‡}

Departament de Química Orgànica Biològica, Institut d'Investigacions Químiques i Ambientals de Barcelona, CSIC, Jordi Girona, 18-26, 08034 Barcelona, Spain, Departament de Química Física i Inorgànica, Universitat Rovira i Virgili, Imperial Tarraco 1, 43005-Tarragona, Spain, and Departament de Química Orgànica i Centre Especial de Recerca en Química Teòrica, Universitat de Barcelona, Martí i Franquès 1, 08028-Barcelona, Spain

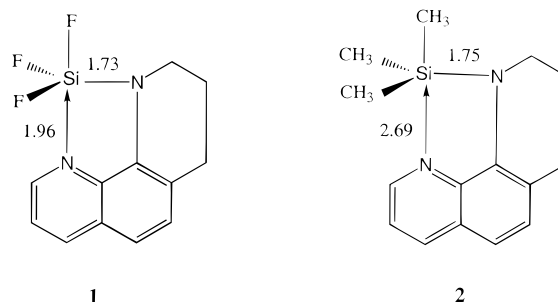
Received June 17, 1999

Using ab initio MP2 and DFT calculations, we have studied the structure of a series of pentacoordinated silicon compounds containing a Si ← N dative bond and the influence of inductive effects on the Si ← N bond. The study includes two series of model systems, namely, Si(NH₃)X_nY_{4-n} (X = OH, Y = H or CH₃; n ranging from 0 to 4) and Si(NH₃)(NH₂)H₂X (X = Cl or H), methyl(2,2',2''-nitrioltriethoxy)silane, methyl(2,2',3-nitriodiethoxypropyl)silane, 8-(trifluorosilylamino)quinoline, 8-(trimethylsilylamino)quinoline, a dimer of Me₂NSiH₂Cl, and a pentamer of Me₂NSiH₃. All these structures have dative Si ← N bonds. The nature of the bonds was analyzed using the Laplacian of the charge density distribution and the natural bond orbital (NBO) partitioning scheme. The calculations show that the dissociation energy of the Si ← N dative bond in the model systems is always lower than 9 kcal mol⁻¹ and that the Si ← N bond length gets shorter as the number of electron-withdrawing groups linked to silicon increases. The different aggregation mode between the dimer of Me₂NSiH₂Cl and the pentamer of Me₂NSiH₃ is also analyzed.

1. Introduction

Very recently Chuit and co-workers¹ and Holmes² reviewed the structure and reactivity of pentacoordinated silicon compounds. Pentacoordination at silicon is usually achieved by coordinating anions to tetracoordinate silicon compounds or by a neutral donor making an intermolecular or intramolecular donation to a silane. The latter usually occurs via nitrogen, oxygen, or sulfur donation, in which case, pentacoordination at silicon is achieved by a dative bond. Haaland³ defines a bond as dative according to its rupture behavior, i.e., if the minimum energy rupture in a neutral diamagnetic molecule proceeds heterolytically to yield neutral diamagnetic species. Haaland also points out that the strength of a dative bond is weaker than the strength of a covalent bond and that the dative bond is very sensitive to the inductive effects of the remaining substituents. This is clearly shown in the dative bond distance of the crystal structures of the related compounds **1** and **2**.^{4,5} If the three electron-withdrawing F atoms on Si are replaced by three

electron-donor CH₃ groups, there is an increase of 0.72 Å in the dative Si ← N bond distance, whereas the length of the covalent Si – N bond increases by only 0.02 Å.



The importance of inductive effects on pentacoordinated silicon compounds was pointed out by Turley et al.⁶ and Boer et al.⁷ in 1969 comparing the Si ← N bond distance between *m*-nitrophenyl(2,2',2''-nitrioltriethoxy)silane (**3a**)⁶ and methyl(2,2',3-nitriodiethoxypropyl)silane (**4**).⁷ Furthermore, a comparison of the X-ray structure of **4** and methyl(2,2',2''-nitrioltriethoxy)silane (**3c**)^{8,9} shows that the substitution of an equatorial O ligand in **3c** by a less electronegative group CH₂ (**4**)

* Corresponding authors. E-mail: anglada@iiqab.csic.es; jmbofill@qo.ub.es; poblet@quimica.urv.es.

[†] Institut d'Investigacions Químiques i Ambientals de Barcelona.

[‡] Universitat Rovira i Virgili.

[§] Universitat de Barcelona.

(1) Chuit, C.; Corriu, R. J. P.; Reye, C.; Young, J. C. *Chem. Rev.* **1993**, *93*, 1371–1448.

(2) Holmes, R. R. *Chem. Rev.* **1996**, *96*, 927–950.

(3) Haaland, A. *Angew. Chem., Int. Ed. Engl.* **1989**, *28*, 992–1007.

(4) Klebe, G.; Hensen, K.; Fuess, H. *Chem. Ber.* **1983**, *116*, 3125.

(5) Klebe, G. *J. Organomet. Chem.* **1985**, *293*, 147.

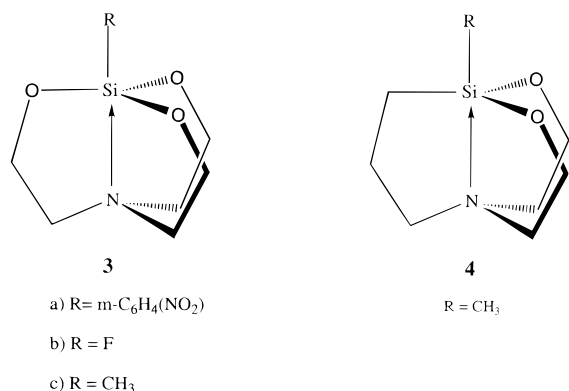
(6) Turley, J. W.; Boer, F. P. *J. Am. Chem. Soc.* **1969**, *91*, 4129–4134.

(7) Boer, F. P.; Turley, J. W. *J. Am. Chem. Soc.* **1969**, *91*, 4134–4139.

(8) Párkányi, L.; Bihátsi, L.; Hencsei, P. *Cryst. Struct. Commun.* **1978**, *7*, 435.

(9) Párkányi, L.; Bihátsi, L.; Hencsei, P. *J. Struct. Chem.* **1991**, *10*, 258.

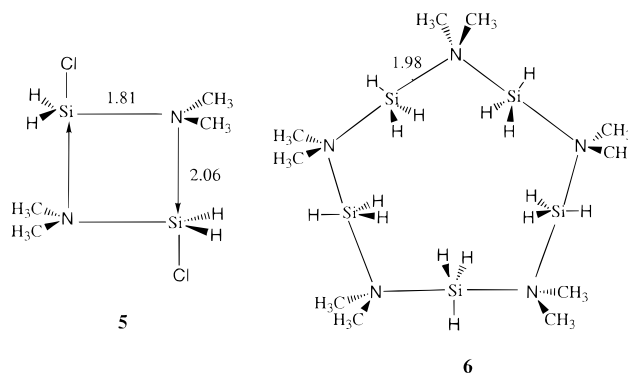
lengthens the Si ← N bond by 0.161 Å. The length of the transannular Si ← N is also very variable in azasilatranes.^{10,11}



The molecular geometries of silatranes **3b** and **3c** have also been determined in the gas phase by electron diffraction techniques.^{12–14} For both silatranes the gas-phase Si ← N bond length is about 0.28 Å longer than in the solid phase. These changes suggest that the Si ← N interaction in the crystal may be influenced by intermolecular forces and provide an insight into the weak nature of the Si ← N bond.^{12–14} Oh and Leopold, who developed a model that accounts for the large gas–solid structure changes,^{15,16} indicated that the dative linkage in the gas phase appears to be intermediate between a van der Waals interaction and a fully formed bond. It is the so-called “partially bonded molecules” model.

Inductive effects can even alter the aggregation mode in the solid phase. For example, Me₂NSiH₂Cl crystallizes as a dimer **5**,^{17–19} in which both units are held together by two dative Si ← N bonds and the Cl atoms occupy axial positions. The non-chlorinated Me₂NSiH₃ is aggregated in a completely different mode in the solid state: it forms a pentamer (**6**).^{19,20} In this case, the three

H atoms bonded to silicon occupy equatorial sites and all N atoms occupy axial sites. The crystal structure of **6** indicates that all silicon–nitrogen bond lengths in the 10-membered ring are equivalent and equal to 1.98 Å.



Several theoretical studies, which focus on pentacoordinated silicon compounds, have been published.^{21–33} The results reported by Schmidt and co-workers²⁹ show that the Hartree–Fock calculated structures for **3b** and **3c** have much longer Si ← N bond distances than the gas-phase structures. Schmidt et al.²⁹ suggest that the electron correlation energy treatments are important if discrepancies between theory and gas-phase experiments are to be removed.

The aim of this paper is to systematically study the inductive effects in some pentacoordinated silicon compounds by means of ab initio and density functional theory (DFT) calculations. First, we discuss the model systems Si(NH₃)X_nY_{4–n} (X = OH, Y = H or CH₃; n ranging from 0 to 4), labeled as **7**, and Si(NH₃)(NH₂)H₂X (X = Cl or H) (**8**), a model that combines in the same structure a dative and a covalent SiN bond. Second, we describe the Si ← N dative bond in the silatran structures **3c** and **4**, the difference between which is that an O is substituted by a CH₂ group in the equatorial position. Third, we discuss 8-(trifluorosily-

(10) Wan, Y.; Verkade, J. G. *J. Am. Chem. Soc.* **1995**, *117*, 141–156.

(11) Wan, Y.; Verkade, J. G. *Organometallics* **1996**, *15*, 5769–5771.

(12) Shen, Q.; Hildebrand, R. L. *J. Mol. Struct.* **1980**, *64*, 257.

(13) Forgács, G.; Kolonits, M.; Hargittai, I. *Struct. Chem.* **1990**, *1*, 245–250.

(14) Rankin, D. W. H.; Robertson, H. E.; Welch, A. J. *Chem. Soc., Dalton Trans.* **1987**, 3035.

(15) Oh, J. J.; LaBarge, M. S.; Matos, J.; Kampf, J. W.; Hillig, K. W., II; Kuczowski, R. L. *J. Am. Chem. Soc.* **1991**, *113*, 4732–4738.

(16) Leopold, K. R.; Canagaratna, M.; Phillips, J. A. *Acc. Chem. Res.* **1997**, *30*, 57–64.

(17) Anderson, D. G.; Blake, A. J.; Cradock, S.; Ebsworth, E. A. V.; Rankin, D. W. H.; Welch, A. J. *Angew. Chem., Int. Ed. Engl.* **1986**, *25*, 107–108.

(18) Anderson, D. G.; Blake, A. J.; Cradock, S.; Ebsworth, E. A. V.; Rankin, D. W. H.; Robertson, H. E.; Welch, A. J. *J. Chem. Soc., Dalton Trans.* **1987**, 3035.

(19) Ebsworth, E. A. V. *Acc. Chem. Res.* **1987**, *20*, 295–301.

(20) Blake, A. J.; Ebsworth, E. A. V.; Welch, A. J. *Acta Crystallogr. Sect. C40* **1984**, 895.

(21) Dieters, J. A.; Holmes, R. R. *J. Am. Chem. Soc.* **1987**, *109*, 1686–1692.

(22) Gordon, M. S.; Davis, L. P.; Burggraf, L. W. *Chem. Phys. Lett.* **1989**, *163*, 371–374.

(23) Dieters, J. A.; Holmes, R. R. *J. Am. Chem. Soc.* **1987**, *109*, 1692–1696.

(24) Damrauer, R.; Burggraf, L. W.; Davis, L. P.; Gordon, M. S. *J. Am. Chem. Soc.* **1988**, *110*, 6601–6606.

(25) Gordon, M. S.; Carroll, M. T.; Jensen, J. H.; Davis, L. P.; Burggraf, L. W.; Guidry, R. M. *Organometallics* **1991**, *10*, 2657–2660.

(26) Greenberg, A.; Plant, C.; Venanzi, C. A. *J. Mol. Struct. (THEOCHEM)* **1991**, *234*, 291–301.

(27) Csonka, G. I.; Hencsei, P. *J. Mol. Struct. (THEOCHEM)* **1993**, *283*, 251–259.

(28) Csonka, G. I.; Hencsei, P. *J. Comput. Chem.* **1994**, *15*, 385–395.

(29) Schmidt, M. W.; Windus, T. L.; Gordon, M. S. *J. Am. Chem. Soc.* **1995**, *117*, 7480–7486.

(30) Gordon, M. S. In *Modern Electronic Structure Theory*; Yarkony, D. R., Ed.; World Scientific: Singapore, 1995; pp 311–344.

(31) Mitzel, N. W.; Losehand, Ü. *Angew. Chem., Int. Ed. Engl.* **1997**, *36*, 2807–2809.

(32) Mitzel, N. W.; Blake, A. J.; Rankin, D. W. H. *J. Am. Chem. Soc.* **1997**, *119*, 4143–4148.

(33) Olsson, L.; Ottosson, C. H.; Cremer, D. *J. Am. Chem. Soc.* **1995**, *117*, 7460–7479.

(34) Frisch, M. J.; Trucks, G. W.; Schlegel, H. B.; Gill, P. M. W.; Johnson, B. G.; Robb, M. A.; Cheeseman, J. R.; Keith, T.; Petersson, G. A.; Montgomery, J. A.; Raghavachari, K.; Al-Laham, M. A.; Zakrzewski, V. G.; Ortiz, J. V.; Foresman, J. B.; Cioslowski, J.; Stefanov, B. B.; Nanayakkara, A.; Challacombe, M.; Peng, C. Y.; Ayala, P. Y.; Chen, W.; Wong, M. W.; Andres, J. L.; Replogle, E. S.; Gomperts, R.; Martin, R. L.; Fox, D. J.; Binkley, J. S.; Defrees, D. J.; Baker, J.; Stewart, J. P.; Head-Gordon, M.; Gonzalez, C.; Pople, J. A. *Gaussian94*; Gaussian, Inc.: Pittsburgh, PA, 1995.

(35) Moeller, C.; Plesset, M. S. *Phys. Rev.* **1934**, *46*, 618.

(36) Frisch, M. J.; Head-Gordon, M.; Pople, J. A. *Chem. Phys. Lett.* **1990**, *166*, 281.

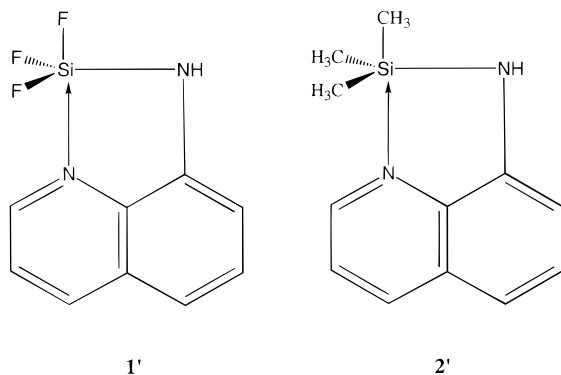
(37) Head-Gordon, M.; Head-Gordon, T. *Chem. Phys. Lett.* **1994**, *220*, 122.

(38) Parr, R. G.; Yang, W. *Density-Functional Theory of Atoms and Molecules*; Oxford University Press: New York, 1989.

(39) Pople, J. A.; Gill, P. M. W.; Johnson, B. G. *Chem. Phys. Lett.* **1992**, *199*, 557.

(40) Johnson, B. G.; Frisch, M. J. *Chem. Phys. Lett.* **1993**, *216*, 133.

laminoquinoline (**1'**) and 8-(trimethylsilylamino)quinoline (**2'**) as models for structures **1** and **2**. Finally, we analyze the Si ← N dative bond in dimer **5** and pentamer **6**.



2. Technical Details

All calculations were carried out with the GAUSSIAN94³⁴ program package. The molecular geometry optimizations were done at the MP2 (second-order Moeller Plesset)^{35–37} and DFT^{38–40} levels of theory. For the dimer **5** and the pentamer **6** only single-point calculations at the crystallographic geometries were performed. In this case, the DFT model was used. In all DFT calculations the B3LYP functional⁴¹ was employed. For compounds **7** and **8** the stationary points were characterized as true minima on the potential energy hypersurface, at both levels of theory, by checking that all eigenvalues of the Hessian matrix were positive. The harmonic vibrational frequencies were also obtained. The calculated MP2/6-31G(d) zero point vibration energies (ZPVE) were scaled by a factor of 0.9670 in order to correct the overestimation of the vibrational frequencies.⁴² All geometry optimizations were carried out using the standard 6-31G(d) basis set.⁴³ Moreover, several of the model systems **7** and **8** were also optimized using the more flexible 6-311++G (d,p) basis set.^{44,45}

The dissociation energies were computed for model compounds **7** and **8** by performing single-point calculations at QCISD(T) (quadratic configuration interaction with singles, doubles, and perturbative estimation of triples method)⁴⁶ level of theory, using the 6-311G(d,p) basis set.⁴⁴ These calculations were made on the geometries optimized at the MP2/6-31G(d) level of theory. All the geometries and energies reported in this work are available as Supporting Information.

The chemical bonds were analyzed by using the natural bond orbital (NBO) partitioning scheme^{47,48} and the topological analysis of the wave function.^{49–51} The AIM-PAC program⁵² was used in this case.

(41) Becke, A. D. *J. Chem. Phys.* **1993**, *98*, 5648.

(42) Scott, A. P.; Radom, L. *J. Phys. Chem.* **1996**, *100*, 16502.

(43) Hariharan, P. C.; Pople, J. A. *Theor. Chim. Acta* **1973**, *28*, 213.

(44) Krishnan, R.; Binkley, J. S.; Seeger, R.; Pople, J. A. *J. Chem. Phys.* **1980**, *72*, 650.

(45) Clark, T.; Chandrasekhar, J.; Spitznagel, G. W.; Shleyer, P. V. *R. J. Comput. Chem.* **1983**, *4*, 294.

(46) Pople, J. A.; Head-Gordon, M.; Raghavachari, K. *J. Chem. Phys.* **1987**, *87*, 5968–5975.

(47) Reed, A. E.; Weinstock, R. B.; Weinhold, F. *J. Chem. Phys.* **1985**, *83*, 735–746.

(48) Reed, A. E.; Curtiss, L. A.; Weinhold, F. *Chem. Rev.* **1988**, *88*, 899–926.

(49) Bader, R. F. W. *Atoms in Molecules. A Quantum Theory*; Clarendon Press: Oxford, U.K., 1990.

(50) Bader, R. F. W. *Chem. Rev.* **1992**, *91*, 893.

(51) Bader, R. F. W.; Popelier, P. L. A.; Keith, T. A. *Angew. Chem., Int. Ed. Engl.* **1994**, *33*, 620.

(52) Biegler-König, F. W.; Bader, R. F. W. *J. Comput. Chem.* **1982**, *3*, 317.

(53) Voronkov, M. G.; Dyakov, V. M.; Kirpichenko, S. V. *J. Organomet.* **1982**, *233*, 1.

3. Results and Discussion

3.1. The Model Systems **7 and **8**.** In the model systems **7**, Si(NH₃)X_nY_{4–n} (X = OH, Y = H or CH₃; *n* ranging from 0 to 4) and **8**, Si(NH₃)(NH₂)H₂X (X = Cl or H) we studied how the inductive effects of different groups influence the Si ← N dative bond. In compounds **7** (labeled as **7a–7l**), we considered combinations of the electron-withdrawing group OH with the electron donor group CH₃ or the substituent H. We also considered the effect of the position (equatorial or axial) of these groups in the molecule. The compounds **8** (labeled as **8a–8c**) are also interesting because in each structure a dative Si ← N coexists with a covalent Si–N bond. These compounds are also models that can be used to study the formation of the dative bond in dimer **5** and pentamer **6**. The most important geometrical parameters of the optimized structures are shown in Figure 1.

Compound **7a** (Si(NH₃)H₄, *n* = 0 and Y = H) is the simplest of the series and had been previously optimized at the MP2 level.²² Figure 1 shows that the geometrical parameters optimized at the MP2 and DFT levels of theory agree quite well. It is worth pointing out that the Si ← N bond length obtained at the MP2 level of theory is long (3.119 Å).

There are six different structures under the general formula Si(NH₃)(OH)_nH_{4–n} (*n* ranges from 1 to 3), all of which have a trigonal bipyramid structure (TBP). They are labeled as **7b–7g** in Figure 1. It is very interesting to observe the change in the Si ← N bond length along this series. According to the geometries optimized at the MP2 level, **7b** (Si(NH₃)H₃(OH)) has a Si ← N bond length of 2.754 Å, while at the opposite end **7g** (Si(NH₃)H(OH)₃) has a Si ← N bond length of 2.032 Å. *The Si ← N bond distance gets shorter as the number of electron-withdrawing groups (OH) increases.* The bond length of **7b–7g** structures decreases by as much as 0.721 Å. Another point of interest is that the dative bond length varies according to the position of the substituent (axial or equatorial) in the pentacoordinated silicon compound. By comparing structures **7b/7c**, **7d/7e**, and **7f/7g**, we find that *the Si ← N bond length is longer when the electron-withdrawing group (OH) is in an axial site.* The most significant change is observed when the structures with a single OH substituent (structures **7b** and **7c**) are compared. In this case, there is a difference of 0.352 Å between both isomers. However, as the number of OH groups increases, the variation in the Si ← N bond distance becomes smaller. If the pentacoordinated silicon compound has three OH substituents (structures **7f** and **7g**), the difference in the dative bond length in both isomers is only 0.083 Å. These results are in accordance with experimental observations in several silatranes, which shows that the presence of electron-withdrawing substituents at the silicon atom (axial position) shortens the SiN distance.^{1,53} For Si(NH₃)H(OH)₃, we also looked for the possibility that the dative Si ← N bond occupies an equatorial position, but the resulting compound turned out to dissociate.

For Si(NH₃)(OH)₄, we found two isomers, which are labeled as **7h** and **7i** in Figure 1. **7h** has a rectangular pyramid-like structure (RP) and **7i** a TB structure. The two isomers have a similar Si ← N bond distance (1.987 and 2.027 Å, respectively).

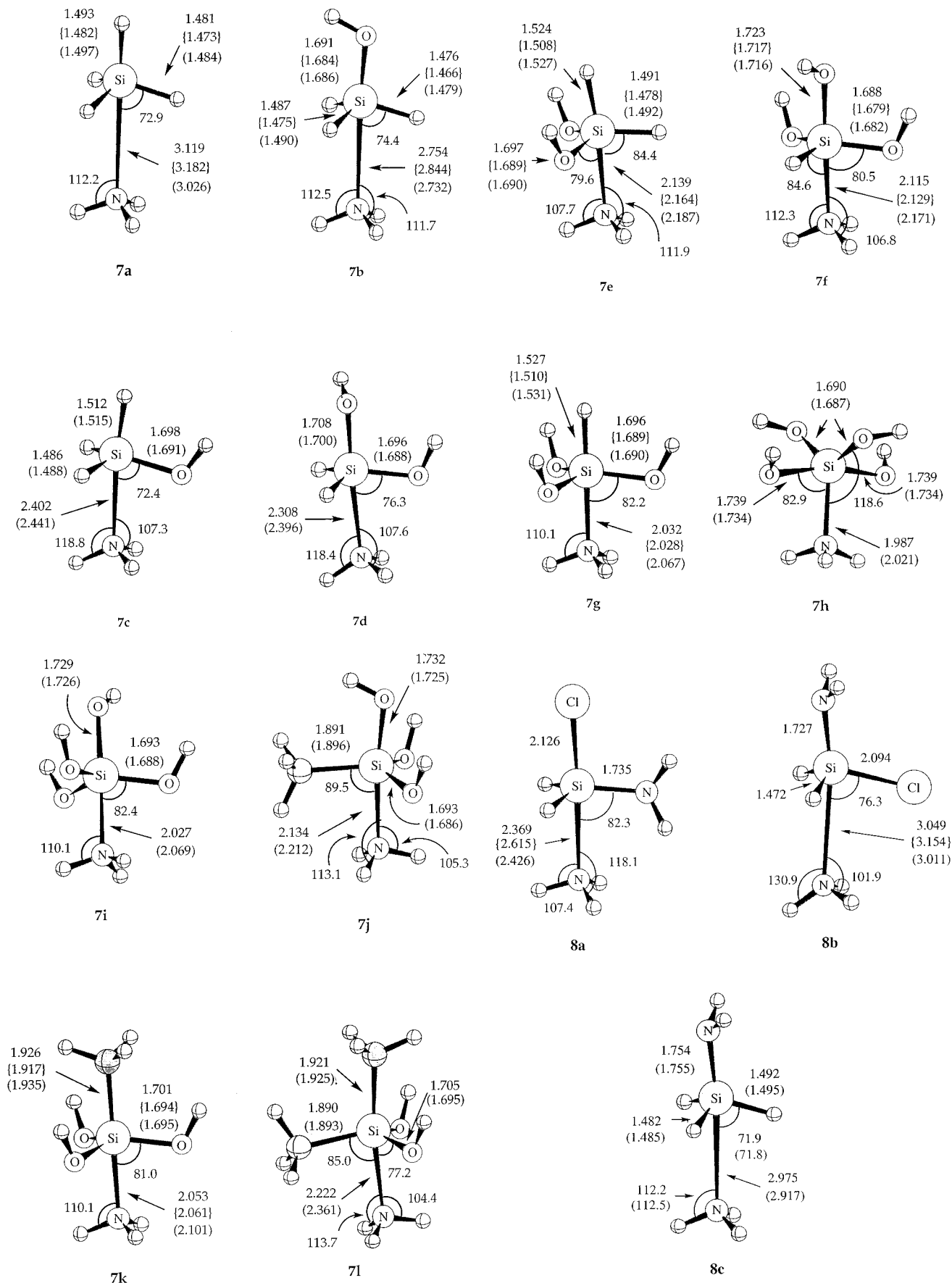


Figure 1. Selected MP2/6-31G(d), MP2/6-311++G(d,p) (in braces), and B3LYP/6-31G(d) (in parentheses) geometrical parameters for model structures **7** and **8**. Distances are in angstroms and angles in degrees.

Finally, there are also six possible structures under the general formula $\text{Si}(\text{NH}_3)(\text{OH})_n(\text{CH}_3)_{4-n}$ (n ranges

from 1 to 3). However, only three of them (**7j**, **7k**, and **7l**) were found to correspond to minima on the potential

energy hypersurface (see Figure 1). **7j** and **7k** are both isomers of $\text{Si}(\text{NH}_3)(\text{OH})_3(\text{CH}_3)$, while **7l** is $\text{Si}(\text{NH}_3)(\text{OH})_2(\text{CH}_3)_2$. The analysis of these structures shows the same general trends pointed out for the $\text{Si}(\text{NH}_3)(\text{OH})_n\text{H}_{4-n}$ series: namely, (a) the Si ← N bond length gets shorter as the number of electron-withdrawing groups (OH) linked to silicon increases (compare **7l** with **7j** and **7k**) and (b) the Si ← N bond distance is longer when the OH group is an axial position.

For $\text{Si}(\text{NH}_3)(\text{NH}_2)\text{H}_2\text{Cl}$, we found two isomers, which are labeled as **8a** and **8b** in Figure 1. Both have a TB structure, but the position of the Cl and NH_2 substituents is different. The dative Si ← N bond always occupies the axial position. Isomer **8a**, which has the Cl in axial position, exhibits the shortest dative Si ← N bond length (2.369 Å). For **8b**, this bond distance is 0.680 Å longer. For $\text{Si}(\text{NH}_3)(\text{NH}_2)\text{H}_3$, the isomer with the NH_2 substituent in axial position (**8c**) is the only one that is stable. The computed Si ← N bond distance is 2.975 Å. This value is 0.221 Å longer than the corresponding distance in **7b**, which possesses only one OH substituent in axial position. Thus, the Si ← N bond length is longer if the ability to withdraw electrons from the remaining substituents is smaller.

Another point of interest is the comparison of the remaining geometrical parameters, such as the SiO bond distance in structures **7**. When the OH groups are in equatorial positions, the SiO bond length remains practically constant in all compounds of the series (**7b**–**7l**) and close to 1.700 Å. However, changes are observed in the SiO bond distance relative to the axial OH group. These changes range from 1.691 Å in **7b** to 1.732 Å in **7j**. So, the axial SiO bond distance increases (although slightly) as the number of OH groups increases. This behavior in the length of the axial bond has also been reported for several pentafluorosilicates.^{1,54–58} Moreover, the pyramidalization of silicon is reduced to approach the pure TBP geometry as the Si ← N gets shorter (see the NSiX angles in Figure 1). It is also interesting to note that the NH_3 group tilts with respect to the axial axis when the silicon substituents in equatorial positions have different electronegativities (compare for instance the different HNSi angles in the model compounds of Figure 1). A similar tilt angle was observed in the gas-phase structure of the trimethylamine–sulfur dioxide complex.¹⁵

Finally, we would like to mention the importance of the basis set. Although Si ← N bond lengths computed using the larger 6-311++G(d,p) basis set agree qualitatively with the results obtained by using the poorer 6-31G(d) basis set for compounds **7**, there are considerable differences when one of the substituents is Cl (differences of 0.246 and 0.105 Å were found for **8a** and **8b**, respectively). These results clearly show that a large basis set is required to study compounds with chlorine as a substituent. Significant differences were also found between the B3LYP and MP2 calculations. The differ-

Table 1. Calculated Bond Properties^a for the Compounds Studied: Si ← N Bond Length, Density, and Laplacian of the Charge Density in the Si ← N Bond, Dipole Moment, ZPVE, and Dissociation Energy for the Model Systems **7 and **8**^d**

com-pound	$r(\text{Si} \leftarrow \text{N})$	ρ_b	$\nabla^2\rho_b$	μ^b	ZPVE	QCISD(T) ^c 6-311G(d,p)
7a	3.119	0.012	0.027	2.94 (2.39)	42.4	3.7 (2.3)
7b	2.754	0.019	0.041	3.84 (3.47)	47.2	5.7 (4.0)
7c	2.404	0.033	0.050	2.75	48.4	4.8 (1.8)
7d	2.316	0.038	0.066	3.47	52.5	6.3 (3.0)
7e	2.139	0.050	0.145	2.16 (1.80)	53.4	7.7 (3.6)
7f	2.115	0.052	0.165	2.72 (2.75)	57.0	7.7 (3.6)
7g	2.032	0.062	0.233	0.97 (0.93)	57.4	8.7 (4.2)
7h	1.988	0.069	0.262	3.58	60.8	-6.3 (-2.2)
7i	2.028	0.063	0.241	1.51	60.1	8.1 (3.7)
7j	2.134	0.051	0.151	2.74	74.6	4.1 (0.2)
7k	2.053	0.060	0.215	0.50 (0.43)	75.2	4.2 (-0.3)
7l	2.221	0.044	0.097	1.49	81.5	1.4 (-2.4)
10a	2.369	0.034	0.050	7.18 (5.66)	52.2	6.0 (3.3)
10b	3.049	0.013	0.029	1.36 (1.00)	50.9	4.6 (3.2)
10c	2.975	0.014	0.032	2.32	48.4	4.1 (5.2)
3c	2.403	0.040	0.033	5.54		
4	2.442	0.038	0.034	4.43		
8	2.073	0.061	0.167	6.69		
9	2.769	0.019	0.043	1.44		

^a Distances are in angstroms. Density and Laplacian of charge density are in atomic units. For ρ_b 1 au = $e/a_0^3 = 6.478 \text{ \AA}^{-3}$, for $\nabla^2\rho_b$ 1 au = $e/a_0^5 = 6.478 \text{ \AA}^{-5}$. Dipole moments are in debyes, and ZPVE and dissociation energy are in kcal mol⁻¹. ^b Values in parentheses are obtained at the MP2/6-311++G(d,p) level of theory. ^c Values in parentheses are ZPVE corrected. ^d All values are computed for the optimized geometries at the M2P/6-31G(d) level of theory.

ences in the Si ← N bond distances range from 0.024 to 0.088 Å (see Figure 1).

Table 1 also collects the computed ZPVE energies and the dissociation energies (D_e) for all the model systems **7** and **8**. The D_e energies were calculated as minus the energy difference between the pentacoordinated silicon compound and the corresponding tetracoordinated silicon compound plus NH_3 . An accurate calculation of D_e should use a larger basis set and the inclusion of basis set superposition errors. However, these are model systems and our aim was only to obtain a qualitative estimation of this value in order to look for the stability trends between the different isomers. The computed dissociation energies are quite low, with values ranging from 1.4 to 8.7 kcal mol⁻¹. The larger dissociation energies correspond to the structures with a higher number of OH substituents. Inclusion of the ZPVE corrections leads to lower dissociation energies, and the compounds **7k** and **7l** appear to be unstable. The isomer **7h**, which has an RP structure, is computed to be less stable than the reactants. These values reflect the weakness of the dative Si ← N bond. The dissociation energy values of some of these compounds are slightly larger than those of typical van der Waals complexes. This agrees with the donor–acceptor character of these compounds^{3,29,33} (see below). To look further into the stability of these model systems, we also considered the influence of the entropic term. The calculated values show that the absolute $T\Delta S$ values computed at $T = 298 \text{ K}$ ⁵⁹ are all greater than the corresponding exothermicity (7–12 kcal mol⁻¹). These values show that

(59) The computed MP2 $T\Delta S$ values are -8.4; -8.6; -10.2; -10.9; -12.1; -11.6; -2.1; -10.9; -12.0; -11.4; -13.4; -12.2; -0.7; -7.4; -7.0 kcal mol⁻¹ for **7a**, **7b**, **7c**, **7d**, **7e**, **7f**, **7g**, **7h**, **7i**, **7j**, **7k**, **7l**, **8a**, **8b**, and **8c**, respectively.

(54) Schomburg, D.; Krebs, R. *Inorg. Chem.* **1984**, *23*, 1378.

(55) Johnson, S. E.; Deiters, J. A.; Day, R. O.; Holmes, R. R. *J. Am. Chem. Soc.* **1989**, *111*, 3250–3258.

(56) Harland, J. J.; Payne, J. S.; Day, R. O.; Holmes, R. R. *Inorg. Chem.* **1987**, *26*, 760.

(57) Schomburg, D. *J. Organomet. Chem.* **1981**, *221*, 137.

(58) Johnson, S. E.; Day, R. O.; Holmes, R. R. *Inorg. Chem.* **1989**, *28*, 3182.

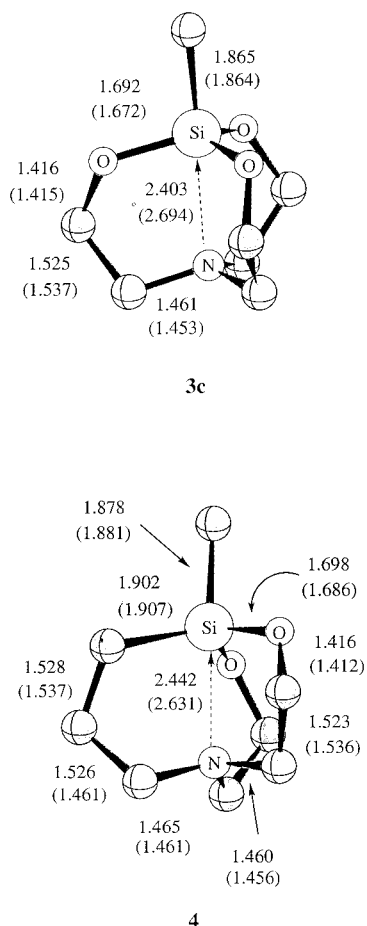


Figure 2. Selected MP2/6-31G(d) and B3LYP/6-31G(d) (in parentheses) geometrical parameters for **3c** and **4**. Distances are in angstroms and angles in degrees. The hydrogen atoms are omitted for the purpose of clarity.

entropy increases because there are more degrees of freedom that arise with the dissociation of the complex. The entropy term at 298 K counterbalances the exothermicity of the formation of the complexes, and therefore, the equilibrium shifts toward the dissociated molecules. By lowering the temperature, the weight of the enthalpic term increases so that more molecules would be complexed. Table 1 also contains the computed dipole moment (μ). It is interesting to note that for the different pairs of isomers (compare **7b/7c**, **7d/7e**, **7f/7g**, **7j/7k**, and **8a/8b**) the larger value corresponds to the isomer with the electron-withdrawing substituent in axial site.

3.2. Structures 3c and 4. The study of **3c** and **4** enables the inductive effects in the Si ← N bond distance to be analyzed because the difference between both compounds is that an equatorial O ligand is replaced by a less electronegative CH₂ ligand. Moreover, the experimental data (gas and solid phase for **3c** and solid phase for **4**)^{7–9,12,13} allow us to check the accuracy of theoretical methods for predicting the geometrical features of compounds with dative Si ← N bonds. Figure 2 shows the most important geometrical parameters for **3c** and **4**. In contrast to previous Hartree–Fock calculations,²⁹ the computed geometrical parameters at the MP2 level for **3c** are in reasonable agreement with the gas-phase values (the computed dative Si ← N bond distance is 2.403 Å and deviates by 0.05 Å from the

experimental gas-phase value¹²). So, the present calculations confirm the importance of including electron correlation. In compound **4**, the dative Si ← N bond length computed at the MP2 level of theory is 2.442 Å, a value that is very close to the one calculated for **3c** at the same level of theory. This dative bond length is 0.112 Å longer than the X-ray value.⁷ From the results of **3c**, we can deduce that the MP2 approach describes the Si ← N bond length quite accurately, so the calculated value for **4** will also be relatively close to the gas-phase value. Our results for **4** show that the difference between the solid and gas-phase dative bond distance (i.e., 0.112 Å) is not as large as for **3c** (0.28 Å).^{12–14} On the other hand, the DFT calculations are of poorer quality, since for **3c** they predict a Si ← N bond length that is 0.24 Å longer than the experimental gas-phase value. This contrasts with the results obtained for the model systems presented above, where in general the Si ← N bond distances computed at MP2 and DFT levels of theory differ by at most 0.09 Å (see Figure 1). Similar results are obtained for **4**, in which the calculated Si ← N bond length at MP2 is 2.442 Å. However, using the DFT method, it is 2.631 Å.

3.3. Structures 1' and 2'. Further experimental evidence of the importance of inductive effects on pentacoordinated silicon compounds is provided by crystal structures **1** and **2**.^{4,5} In structure **1**, three fluorine atoms occupy two of the equatorial and one of the axial sites, whereas the other two coordination sites are occupied by two nitrogen atoms. The presence of the dative bond in the axial site is in agreement with the MP2 calculations for structures **7**, which show that if the dative bond occupies an equatorial site, the Si ← N bond dissociates. An interesting feature of structure **1** is that a relatively short Si ← N bond (1.969 Å) coexists with a covalent interaction between the silicon atom and the amine nitrogen in an equatorial position.

As pointed out in the Introduction, we have simplified structures **1** and **2** and use model structures **1'** and **2'**. The most important optimized geometrical parameters are displayed in Figure 3. The calculations were carried out at both MP2 and DFT levels of theory. The computed MP2 Si ← N bond lengths are 2.073 and 2.769 Å for **1'** and **2'**, respectively (the DFT method predicts Si ← N bond lengths of 2.087 and 2.966 Å). These computed MP2 dative bond lengths differ from the experimental X-ray values of the related compounds **1** and **2** by 0.11 and 0.08 Å. However, we should compare the calculated values with the experimental gas-phase results, which are unavailable for compounds **1** and **2**. Taking into account the increase of 0.28 Å observed in the Si ← N bond distance between the X-ray and the gas-phase structures of **3b** and **3c**,^{8,9,12–14} we believe that the deviation between the computed and experimental dative bond lengths should be smaller. The discrepancies for the other parameters are notably smaller (see Figure 3).

3.4. Bond Analysis. The study of the bond properties is based on the topological analysis of Bader and on the natural bond orbital procedure (NBO). The topological properties of a bond are characterized by the existence of a bond critical point (bcp) at the equilibrium geometry and the values of the electron density (ρ_b) and its Laplacian ($\nabla^2\rho_b$) at the bcp.^{49–51} Table 1 collects the

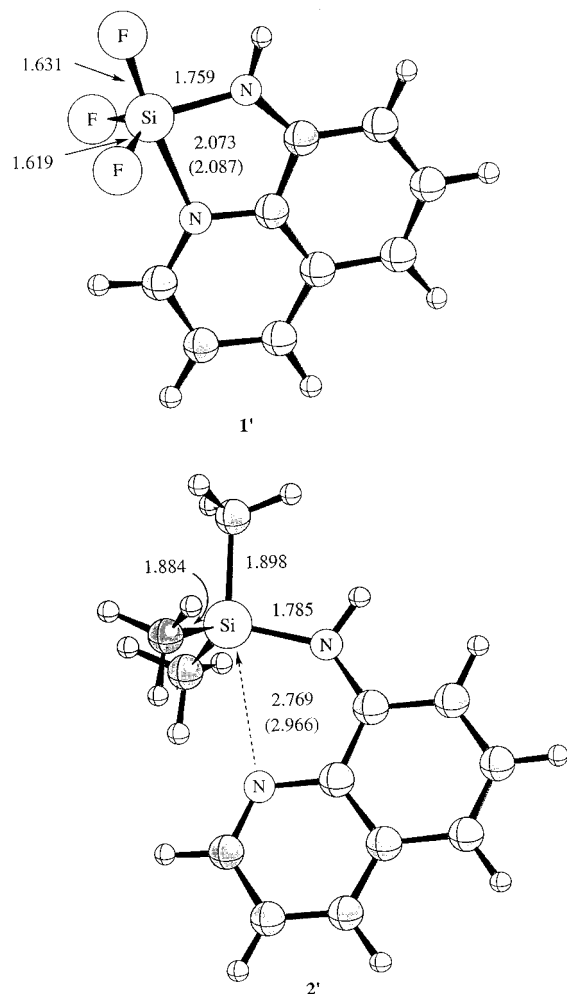


Figure 3. Selected MP2/6-31G(d) and B3LYP/6-31G(d) (in parentheses) geometrical parameters for **7** and **8**. Distances are in angstroms and angles in degrees.

computed density and the Laplacian of the charge density in all the dative Si ← N bonds considered. This table shows that all the Si ← N bonds have positive values of $\nabla^2\rho$, which is characteristic of “closed shell” interactions. Moreover, an inverse correlation is found between ρ_b and the corresponding bond length. Structure **7b** has a very long Si ← N bond (2.756 Å), and the values of ρ_b and $\nabla^2\rho_b$ are quite small (0.012 and 0.027 au, respectively, see Table 1 and Figure 1). Substitution of the three hydrogen atoms by three OH groups in **7b** leads to a Si ← N bond length of 2.027 Å (**7i**). Despite this dramatic shortening, the value of $\nabla^2\rho_b$ remains positive, which emphasizes the closed shell nature of the silicon–nitrogen interaction. Moreover, the remaining compounds shown in Table 1 have the same trends, and they all have positive $\nabla^2\rho_b$ values. This indicates that all the compounds considered have a closed shell interaction between NH₃ and the silicon moiety, which is characteristic of a dative bond. Consequently, *the shortening of the dative bonds in the different compounds is not caused by a change in the nature of the bond.* This analysis agrees with the results reported by Jonas et al.,⁶⁰ who show that strong dative bonds are not necessarily covalent. Moreover, the values of the

Laplacian of the charge density displayed in Table 2 give support to Haaland’s bonding model.³

We shall now discuss cage effects in silatranes. The Laplacians of the charge density at the Si ← N critical points are 0.033 and 0.038 au for **3c** and **4**, respectively, which is similar to the corresponding value of the model **7b** (see Table 1). However, structures **3c** and **4** in some way resemble **7k** and **7l** since all four structures have a methyl group in axial positions. Moreover, the equatorial substituents are three oxygen atoms for **3c** and **7k** and two oxygen atoms and one carbon atom for **4** and **7l**, respectively. Despite this similarity, the MP2 Si ← N bond distances present notable differences. Whereas the silicon–nitrogen bond lengths are 2.053 and 2.222 Å for **7k** and **7l**, respectively, the computed values of 2.403 and 2.442 Å for structures **3c** and **4** are clearly longer in the silatranes, and these differences suggest that cage effects may be important in silatranes.

Further information is provided by the NBO analysis. Table 2 shows the natural occupations on the Si atom, the natural charges on Si and on the dative N atoms, the $r(\text{Si}-\text{N})$ bond distance, and charge transfer between NH₃ and the silicon moiety. There is an inverse linear correlation between the charge transfer and the dative Si ← N bond length. For instance, the substitution of the four H ligands in **7a** by four OH ligands in **7i** reduces the silicon–nitrogen bond length by 1.091 Å, while the charge transfer from the NH₃ to the silicon moiety increases by 0.145 *e*. Moreover, if we compare the structures of the pairs of isomers **7b/7c**, **7d/7e**, and **7f/7g**, we observe (see Table 2) a larger charge transfer when the OH substituents are in equatorial sites. This explains that the shortening of the dative Si ← N bond length in each pair of isomers depends on the sites of the substituents. (See also Figure 1 and the discussion in section 3.)

As Olsson et al. pointed out,³³ charge transfer occurs from the electron lone pair on N to the σ^* (SiX) orbital (X being the substituents). The acceptor ability of the silicon compound depends on the electronic nature, the number, and the sites of the substituents linked to silicon (compare for instance in Table 2 the computed NBO charge transfer in **7b** and **7c**, which have only one OH substituent, and **7f** and **7g**, which have three OH substituents). The NBO analysis also suggests that there is a formal $sp^3 \rightarrow sp^2$ hybridization change on silicon as the pentacoordinated compound is being formed, and this hybridization change increases as the number of OH substituents increases, that is, as the Si ← N gets shorter. As a result, the SiX_{axial} overlap reduces more than the SiX_{equatorial}, giving a slightly lower bond order for the SiX_{axial} bond. Moreover, the NBO analysis shows that the σ^* (SiX) orbital corresponding to the sp^2 hybridization (equatorial sites) allows a slightly greater occupation than the axial one, indicating a larger charge transfer in those isomers with more OH substituents placed in equatorial sites. The geometrical parameters of the equatorial substituents in the model systems also reflect this hybridization picture. Thus, for instance in compound **7i**, the computed equatorial OSiO angles are 116.7 and 119.2 Å, respectively, whereas in the tetracoordinated Si(OH)₄ compound the calculated OSiO angles are 105.8 Å. This formal hybridization change in the formation of the

(60) Jonas, V.; Frenking, G.; Reetz, M. T. *J. Am. Chem. Soc.* **1994**, *116*, 8741–8753.

Table 2. Si ← N Bond Length (in Å) and Results of the NBO Analysis for the Pentacoordinated Silicon Compounds Computed at the MP2/6-31G(d) Level of Theory^a

compound ^b		<i>r</i> (Si ← N)	Si natural occupation			NBO charges		charge transfer
			3s	3p	3d	Si	N	
7a	H ₄	3.119 (3.182)	1.03	2.17	0.07	0.741 0.784	-1.122 (-1.024)	0.024 (0.016)
7b	H ₃ (OH) ax	2.754 (2.844)	0.94	1.70	0.06	1.281 (1.290)	-1.123 (-1.022)	0.046 (0.035)
7c	H ₃ (OH)	2.404	0.91	1.72	0.06	1.289	-1.120	0.091
7d	H ₂ (OH) ₂ ax	2.316	0.82	1.39	0.07	1.698	-1.125	0.102
7e	H ₂ (OH) ₂	2.139 (2.164)	0.78	1.42	0.07	1.707 (1.641)	-1.118 (-0.986)	0.146 (0.164)
7f	H(OH) ₃ ax	2.115 (2.129)	0.67	1.18	0.07	2.054 (1.960)	-1.124 (-0.985)	0.146 (0.174)
7g	H(OH) ₃	2.032 (2.028)	0.64	1.21	0.07	2.061 (1.953)	-1.119 (-0.974)	0.175 (0.213)
7h	(OH) ₄	1.988	0.54	1.00	0.07	2.365	-1.138	0.189
7i	(OH) ₄ ax	2.028	0.53	1.01	0.06	2.365	-1.127	0.169
7j	(CH ₃)(OH) ₃ ax	2.134	0.59	1.03	0.06	2.280	-1.125	0.142
7k	(CH ₃)(OH) ₃	2.053 (2.061)	0.57	1.06	0.06	2.281 (2.108)	-1.119 (-0.971)	0.168 (0.205)
7l	(CH ₃) ₂ (OH) ₂	2.221	0.64	1.09	0.05	2.186	-1.115	0.130
10a	(NH ₂)H ₂ Cl ax	2.369 (2.615)	0.88	1.61	0.07	1.405 (1.353)	-1.124 (-1.020)	0.104 (0.067)
10b	(NH ₂)H ₂ Cl	3.049 (3.154)	0.90	1.63	0.07	1.380 (1.336)	-1.130 (-1.035)	0.024 (0.012)
10c	(NH ₂)H ₃	2.975	0.93	1.80	0.06	1.188	-1.120	0.031
3c		2.403	0.60	1.00	0.06	2.315	-0.573	
4		2.442	0.65	1.05	0.05	2.215	-0.567	
8		2.073	0.52	0.96	0.07	2.418	-0.524	
9		2.769	0.71	1.23	0.04	1.998	-0.446	

^a Values in parentheses correspond to MP2/611++G(d,p) calculations. ^b ax means that the substituent is placed in axial position.

pentacoordinated compound also agrees with the simple MO diagram based on the three-center, four-electrons model (3c4e) with the consequent availability of the 3p_z orbital of silicon for the dative bond.^{29,61} To sum up, these changes in the silicon hybridization explain the trends discussed in the section above: the longer SiX bond when X is in an equatorial site; the lowering of the silicon pyramidalization as Si ← N gets shorter and the fact that NH₃ always occupies an axial site. Moreover, these trends resemble the electronic situation described in the nucleophilic substitution reactions (S_N2 reactions). For carbon compounds, the pentacoordinated structure corresponds to the transition state of the reaction (the carbon atom adopting a sp² hybridization),⁶² whereas for silicon compounds, the pentacoordinated structure corresponds to a minimum in the potential energy surface.^{23,24} In this respect, Anderson et al.¹⁷ said textually, "We may regard dimer **5** as a frozen intermediate in an S_N2 reaction."

3.5. Dimer 5 versus Pentamer 6. This last section will analyze the Laplacian of the electronic charge density distribution of related silylamines. As we have mentioned above, Me₂NSiH₂Cl crystallizes as dimer **5**, and the two-monomer units are held together by two dative Si ← N bonds in the solid.^{17,18} In dimer **5**, the coordination around the silicon atoms is bipyramidal, with the long (2.06 Å) and short (1.81 Å) Si–N bonds in the axial and equatorial positions, respectively. Substitution of the Cl atom by H leads to an important change in the solid state where Me₂NSiH₃ crystallizes as a pentamer (**6**).^{19,20} In **6** the coordination of the silicon is also bipyramidal, but the nitrogen atoms occupy the

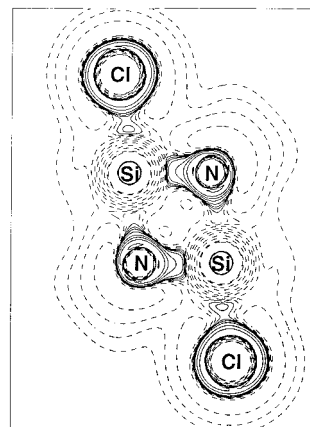


Figure 4. Plots of $\nabla^2\rho$ in a plane containing the Si–N bonds for the dimer **5**. Dashed lines correspond to $\nabla^2\rho > 0$ (regions of charge depletion) and solid lines to $\nabla^2\rho < 0$ (regions of charge concentration).

two axial positions and the two Si–N bond distances are equivalent (1.98 Å). For both structures, we have only carried out DFT single-point calculations at the crystal geometries. The Kohn–Sham molecular orbitals were used to determine the Laplacian of charge density distribution.

Figure 4 shows a map of the Laplacian of charge density for **5** in a plane, which contains the Si, N, and Cl atoms. It can be seen from this figure that the Laplacian of the charge density of the Si–N_{equatorial} bonding region has a very large covalent contribution, with a charge concentration region linking the Si and N atoms. The presence of a maximum of charge concentration in the vicinity of the N_{axial} facing a depopulated region of the Si is a strong indication that the interaction between Si and the axial N should be classified as dative. On the other hand, the map of $\nabla^2\rho$

(61) Iwamiya, J. H.; Maciel, G. E. *J. Am. Chem. Soc.* **1993**, *115*, 6835–6842.

(62) Dewar, M. J. S.; Dougherty, R. C. *The PMO Theory of Organic Chemistry*; Plenum Press: New York, 1975.

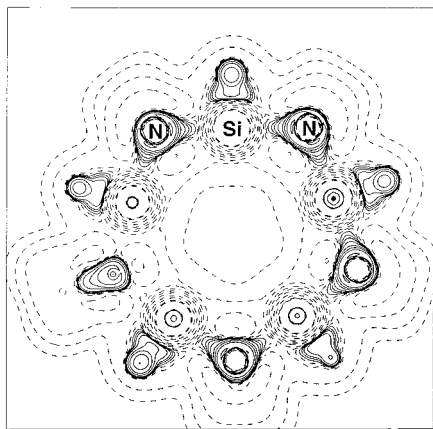


Figure 5. Plots of $\nabla^2\rho$ in a plane containing the Si–N bonds for the pentamer **6**. Dashed lines correspond to $\nabla^2\rho > 0$ (regions of charge depletion) and solid lines to $\nabla^2\rho < 0$ (regions of charge concentration).

for the pentamer structure **6** (Figure 5) shows that the valence shell of the charge concentration of the N atom of each amine fragment has pronounced maxima in the bonding region of the Si–N bonds. This maximum, together with the lack of a charge concentration region connecting N and Si, provides evidence that *the five Me_2NSiH_3 units are held together by 10 dative bonds*. The distinct character of the SiN bonds in dimer **5** (one covalent and one dative) and in pentamer **6** (all dative) may be rationalized taking into account the formal hybridization change ($\text{sp}^3 \rightarrow \text{sp}^2$) that occurs in forming the pentacoordinated silicon compound. In pentamer **6**, both nitrogen substituents occupy axial sites and interact with silicon through its $3p_z$ orbital so both N substituents become equivalent and may have dative character. However, in dimer **5**, one N substituent occupies an axial site and can form a dative bond, while the other N substituent is in an equatorial site and interacts with the silicon atom through an sp^2 -like hybrid orbital, forming a covalent bond.

According to Ebsworth,¹⁹ the presence of two nitrogens occupying axial sites in $(\text{SiH}_3\text{NMe}_2)_5$ is the origin of the pentameric aggregation in this compound. Calculations carried out on the model system $\text{Si}(\text{NH}_3)(\text{NH}_2)\text{H}_3$ support this hypothesis, since only the isomer with the NH_2 substituent in an axial site (**8c**) is stable. In dimer **5**, $(\text{Me}_2\text{NSiH}_2\text{Cl})_2$, the Cl substituents occupy axial sites and the presence of N ligands in an equatorial site makes the four-membered ring feasible. This aggregation mode agrees with the results on the model system $\text{Si}(\text{NH}_3)(\text{NH}_2)\text{H}_2\text{Cl}$, in which the most stable isomer (**8a**) (see the previous section) also has the Cl and NH_2 substituents in axial and equatorial positions, respectively. However, the isomer with Cl in equatorial and NH_2 in the axial position (**8b**) is also stable. Therefore, from a structural point of view, the corresponding isomer could also crystallize as a pentamer. Perhaps in this case, the preference for a dimeric aggregation could be understood from the larger dipole moment expected for the compound with the Cl substituent in an axial site (compare dipole moments for **8a** and **8b** in Table 1). This would favor the dimer according to the model of Oh et al. and Loepold et al.^{15,16}

Finally, the dimeric and pentameric aggregation mode of $\text{Me}_2\text{NSiH}_2\text{Cl}$ and $\text{Si}(\text{NH}_3)(\text{NH}_2)\text{H}_3$ is also in ac-

cordance with the similarities to the $\text{S}_{\text{N}}2$ reactions pointed out above. In these reactions, the leaving group always occupies an axial site in the “pentameric” transition state structure. Thus, for $\text{Me}_2\text{NSiH}_2\text{Cl}$, the chlorine atom is a better leaving group than the amine group, and consequently it prefers an axial site, whereas if we compare NH_2 and H, the amine is the best leaving group.

4. Summary and Conclusions

From the results obtained in the present research, we would like to emphasize the following points.

(1) The dative Si–N bond length is very sensitive to inductive effects. This is clearly seen in the study of model systems **7**, where we observed that the Si–N bond distance varied by as much as 0.723 Å between structures **7b** and **7g**. The Si–N bond distance gets shorter as the number of electron-withdrawing groups linked to silicon increases. We also observed that the Si–N bond length is longer when an electron-withdrawing group bonded to silicon is in an axial position than when it occupies an equatorial site. The same trends are observed for the remaining compounds studied and are in accordance with experimental observations in several pentacoordinated silicon compounds.^{1,8–11}

(2) In general, the MP2/6-31G(d) optimized parameters for **3c** agree quite well with the experimental gas-phase values. The greatest discrepancy appears in the dative bond and is less than 0.05 Å. The comparison of the **3c** and **4** structures with **7k** and **7l**, respectively, suggests that the Si–N bond length in silatranes may be affected by cage effects. In general, the results obtained at DFT and MP2 levels are similar, with the exception of the Si–N bond lengths in compounds **3c**, **4**, and **2'**, for which the DFT method predicts values about 0.2 Å longer.

(3) The computed dissociation energies for model systems **7** and **8** are in the 1.4–8.7 kcal mol^{−1} range and are even lower if the ZPVE are taken into account. The larger dissociation energies were found for the compounds with the most electron-withdrawing substituents. The highest dipole moments computed for the different pairs of isomers for **7** and **8** were for the isomer with the electron-withdrawing substituent in an axial site.

(4) The topological analysis of the wave function indicates the presence of a bond critical point in the Si–N bond for all the systems studied. The positive value of the Laplacian of the charge density emphasizes the closed shell nature of the interaction between nitrogen and silicon that is characteristic of dative bonds. So, the change in the dative bond length in the different compounds is not caused by a change in the nature of the bond.

(5) The NBO analysis shows us that the formation of a pentacoordinated silicon compound involves a formal $\text{sp}^3 \rightarrow \text{sp}^2$ hybridization change on silicon. This leads to the formation of the dative Si–N bond. These neutral pentacoordinated silicon compounds are charge-transfer complexes, and we found an inverse linear relationship between the charge transfer among the NH_3 and silicon moieties and the dative bond length.

(6) The analysis of the SiN bonds shows that in dimer **5** a dative and a covalent SiN bond coexist, whereas in pentamer **6** all the SiN bonds can be classified as dative. This is a consequence of the sites that the two nitrogen substituents occupy around the silicon atom (axial and equatorial in the dimer and all axial in the pentamer), according to the hybridization picture provided by the NBO analysis. The different aggregation mode of Me₂NSiH₂Cl (as dimer) and Me₂NSiH₃ (as pentamer) is explained as a structural requirement, as has been pointed out in the literature.^{19,20}

Acknowledgment. This research was supported by the Dirección General de Investigación Científica y Técnica (DGICYT Grants PB95-0278-C02-01, PB95-0278-C02-02, and PB95-0639-C02-02). The calculations

were performed in the IMB-SP2 at the CESCO, in the Fujitsu VP2400 at the CESGA, and in several workstations at the U.R.V. One of us, R.C., wishes to thank the C.I.R.I.T. (Generalitat de Catalunya, Spain) for financial support. The authors also want to thank Professor Santiago Olivella for his valuable suggestions and continuous encouragement.

Supporting Information Available: Tables containing Cartesian coordinates and total energies of all structures reported in this paper. This material is available free of charge via the Internet at <http://pubs.acs.org>. dAll values 177408n page the optimized geometries at the MP2/6-31G(d) level of theory.

OM9904697